



# Surface pressure and elevation correction from observation and multiple reanalyses over the Tibetan Plateau

Qinglong You<sup>1</sup> · Yuntao Bao<sup>2</sup> · Zhihong Jiang<sup>2</sup> · Nick Pepin<sup>3</sup> · G. W. K. Moore<sup>4</sup>

Received: 10 August 2018 / Accepted: 17 July 2019 / Published online: 23 July 2019  
© Springer-Verlag GmbH Germany, part of Springer Nature 2019

## Abstract

Surface pressure reflects the deep structure of the overlying atmosphere, and is recognized as an indicator of climate change. In this study, observed surface pressure at 71 stations over the Tibetan Plateau (TP) during 1979–2013 is analyzed and compared with monthly means from multiple reanalyses (NCEP1, NCEP2, ERA-Interim, MERRA and JRA55). During the studied period, surface pressure from both observations and the reanalyses increases slowly up until the mid-2000s but shows a decrease afterwards, leading to a recent fall in pressure. However, the surface pressure over the TP in spring has increased, probably explained by the thermal condition such as diabatic heating change. Observations and the multiple reanalyses are positively correlated at most locations indicating that reanalyses reproduce the interannual variation and long-term trend of observed surface pressure fairly well. Despite high inter-annual correlation, trend magnitudes over 1979–2013 are varied, with observations showing decreased pressure at most stations, but reanalyses showing increases in many cases. Compared with observations however, surface pressures from all reanalyses are underestimated usually by about 3–6%. There are significant positive correlations between surface pressure bias and elevation bias, suggesting that overestimation of elevation partially explains the surface pressure bias. A topographical correction method using the hydrostatic equation is therefore conducted and more than 90% of the biases of the reanalyses can be eliminated. Overall, this study points to the importance of better analyzing the importance of topography in the western TP to enhance understanding of reanalysis uncertainties in this region.

**Keywords** Tibetan Plateau · Surface pressure · Multiple reanalyses · Trend

## 1 Introduction

Due to the extensive area of high terrain, the Tibetan Plateau (TP) exerts a strong influence on regional and global atmospheric circulation and climate, particularly in central and eastern Asia through both mechanical and thermal forcing (Duan et al. 2012; Liu et al. 2009; Wu et al. 2015;

Yang et al. 2011, 2014, You et al. 2015a, 2017). In summer, the TP serves as a significant heat source, and plays a unique role in controlling the development of the Asian summer monsoon and resultant weather systems over the whole of China. This has been examined through numerical simulations, numerous data analyses and theoretical studies (Duan et al. 2012; Duan and Wu 2005; Rangwala et al. 2010; Wu et al. 2015; Yanai and Li 1994; Yanai et al. 1992; You et al. 2013c, 2015a). Surface heating can trigger deep convection above the TP which supports exchange of water vapor and air pollutants between the troposphere and stratosphere (Fu et al. 2006). In winter, the TP acts as an elevated cold land surface for snow/ice accumulation and glacier development, and provides a water source for the Asian population (Barnett et al. 2005). Previous studies have shown a close relationship between winter snow/glacier accumulation in the TP and the intensity of the following Indian/East Asian summer monsoon (Hahn and Shukla 1976; Moore 2012; Wu and Qian 2003). For example there are clear positive correlations between snow

✉ Qinglong You  
yqingl@126.com

<sup>1</sup> Department of Atmospheric and Oceanic Sciences and Institute of Atmospheric Sciences, Fudan University, Shanghai 200438, China  
<sup>2</sup> Key Laboratory of Meteorological Disaster, Ministry of Education (KLME), Nanjing University of Information Science and Technology (NUIST), Nanjing 210044, China  
<sup>3</sup> Department of Geography, University of Portsmouth, Portsmouth PO1 3HE, UK  
<sup>4</sup> Department of Physics, University of Toronto, Toronto, ON, Canada

cover over the TP and subsequent summer rainfall over the middle and lower reaches of the Yangtze River valley (central China) (Wu and Qian 2003). However, long term climate and cryospheric changes over the TP have altered atmospheric and hydrological cycles and reshaped the local environment (Kang et al. 2010; Yang et al. 2011, 2014; You et al. 2013a, b). Our understanding of climate change over the TP has been significantly advanced in the recent decades due to improvements in both observational data and numerical models (Cai et al. 2017; Cuo et al. 2013; Kang et al. 2010; Liu et al. 2009; Wu et al. 2015; Yang et al. 2014). In addition to models and observations, reanalyses are also an important data source, and are used extensively in the study of weather and climate, due to their consistent temporal and spatial resolution (Dee et al. 2011; Kobayashi et al. 2015; Rienecker et al. 2011). However, reanalyses require systematic evaluation of their quality before extending their application (Bao and Zhang, 2013; Ma et al. 2008; You et al. 2013a).

Surface pressure is an easily measured field and relatively insensitive to local-scale features, and can therefore be representative of large-scale atmospheric conditions. Furthermore, the first source of variation in surface pressure comes from topography, which is location-dependent (Compo et al. 2006; Hahn and Shukla 1976; Moore 2012; You et al. 2017). The annual mean cycle and inter-annual variability of surface pressure can be analyzed to depict the state of the climate system (Chen et al. 1997; Cullather and Lynch 2003; Han et al. 2010; Trenberth 1981; van den Dool and Saha 1993; Zishka and Smith 1980). Previous studies show that changes in surface pressure are associated with a wide range of atmospheric phenomena, such as mesoscale gravity waves, convective complexes, and synoptic disturbances (Jacques et al. 2015; Koppel et al. 2000). In addition, compared with temperature and wind measurements, surface pressure observations have fewer siting and measurement issues (Mass and Madaus 2014), which makes them readily assimilated into operational models (Mass and Madaus 2014; Wheatley and Stensrud 2010). Assimilation of surface pressure observations is non-trivial in high-altitude terrain, and the adjustment to station altitude is of great importance when considering the pressure observations (Ingleby 2015). Therefore, numerous studies have relied on pressure observations to catalogue and examine climate change (e.g., Toumi et al. 1999), changes in atmospheric or oceanic circulation (e.g., Han et al. 2010), synoptic storm tracks (e.g., Zishka and Smith 1980) and the total mass of the atmosphere (e.g., Trenberth 1981). Changes in surface pressure not only test the reliability of climate models but also facilitate understanding of the atmosphere as a whole (Van Wijngaarden 2005) because surface pressure reflects the overlying structure of the whole atmospheric column (Mass and Madaus 2014).

Considerable efforts to obtain more reliable estimates of surface pressure have been performed on global and regional scales (Chen et al. 1997; Moore 2012; Toumi et al. 1999; Trenberth et al. 1987; Van Wijngaarden 2005), including studies of the Hadley Center historical gridded global monthly mean sea level pressure (HadSLP) (Allan and Ansell 2006), the Arctic (Gillett et al. 2003), the Canadian Arctic (Gillett et al. 2003; Van Wijngaarden 2005), the United States (Jacques et al. 2015; Koppel et al. 2000), the Southern Ocean and Antarctica (Hines et al. 2000), the Tibetan Plateau (Moore 2012; You et al. 2017), and the Indian Ocean (Gillett et al. 2003). It has been shown that surface pressure in the Arctic region has decreased by 4 hPa during winter over the period 1968–1997 (Gillett et al. 2003). Over the Canadian Arctic in winter, the surface pressure has decreased by 3–4 hPa during 1948–1998 (Gillett et al. 2003), confirmed by the fact that surface pressure during 1953–2003 has shown a statistically significant decrease in the same region (Van Wijngaarden 2005).

Over the TP, surface pressure is low/high when surface temperature is low/high, partly because of the high elevation. This is in contrast to many lowland areas, particularly on mid-latitude continents where the reverse can be the case because of the association of anticyclones with cold air in winter (Saha et al. 1994; van den Dool and Saha 1993). Several studies have documented the variability of surface pressure over the TP, with particular interest in patterns during the south Asian monsoon (Wu et al. 2015; Yanai et al. 1992) and TP monsoon (Kang et al. 2010). These questions are crucial to understanding not only ground/surface climate change but also the structure of the upper-air over the TP. Surface pressure can be used to yield a reasonable approximation of circulation where flow is barotropic, in turn allowing development of indices representing amplitudes and phases of various atmospheric modes (Compo et al. 2006; Trenberth et al. 1987).

In this study, the variability of surface pressure across the TP is analyzed using monthly means from station observations and multiple reanalyses. The purpose of this study is to address the following questions:

- (1) What is the variability of observed surface pressure over the TP?
- (2) How well do the multiple reanalyses reproduce the observed pressure across the TP?
- (3) What are the reasons for discrepancies between observations and reanalyses?

This study is organized as follows: Sect. 2 describes the datasets and methods. In Sect. 3.1, the climatology and variability of surface pressure over the TP are presented. In Sect. 3.2, the correlation between surface pressure bias and elevation bias over the TP is analyzed and

the corrections of surface pressure biases over the TP are performed. Section 3.3 shows the trend of surface pressure after topography correction over the TP. Section 3.4 analyzes the possible mechanism for surface pressure changes over the TP. Section 4 summarizes the discussion and conclusions.

## 2 Data and methods

### 2.1 Surface pressure from observation and multiple reanalyses

Observed monthly surface pressure at 71 stations (Fig. 1) is provided by the National Meteorological Information Center, China Meteorological Administration (NMIC/CMA). Stations are chosen according to selection procedures described

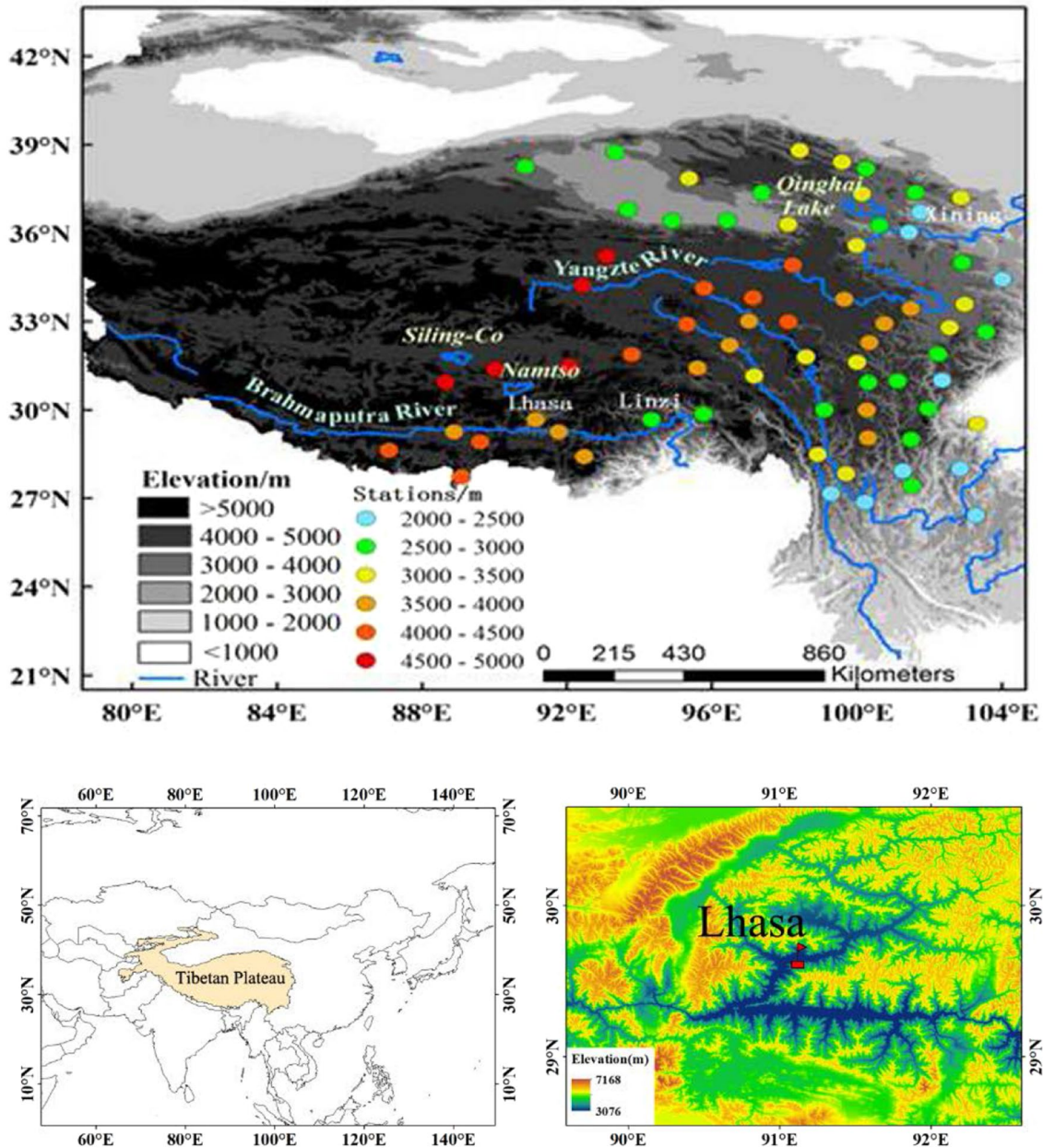


**Fig. 1** The distribution of 71 stations with elevation information over the Tibetan Plateau. Most stations over the Tibetan Plateau are situated predominantly in flat areas and lower mountain valleys on the

southern and eastern parts of the Tibetan Plateau. Lhasa station is shown as an example

in previous papers (You et al. 2008a, b). Only stations above 2000 m were selected. The period 1979–2013 is examined. We believe that the surface pressure at 71 stations is independent from the reanalysis products. In the future, such verifications will become possible if all reanalysis producers publish the observations used along with the reanalysis feedback.

Monthly surface pressures from five reanalyses are used, and more details are described in Table 1. These include the National Centers for Environmental Prediction (NCEP)-National Center for Atmospheric Research (NCAR) Reanalysis Project (NCEP1 hereafter) (Kalnay et al. 1996; Kistler et al. 2001); the NCEP-Department of Energy (DOE) Reanalysis Project (NCEP2) (Kanamitsu et al. 2002); the European Centre for Medium-Range Weather Forecasts (ECMWF) Interim Reanalysis (ERA-Interim) (Dee et al. 2011); the Japan Meteorological Agency (JMA) 55 year Reanalysis Project (JRA55) (Kobayashi et al. 2015); and the National Aeronautics and Space Administration (NASA) Modern-Era Retrospective Analysis for Research and Applications (MERRA) (Rienecker et al. 2011). It should be noted that there are other reanalyses, but due to lack of time we could not consider them all. We hence decided to focus the work on a few widely-used reanalysis products, because they are well-documented. These products are known to contain limitations, and some products have been replaced by more recent products. For example, both NCEP1 and NCEP2, ERA-Interim, and MERRA were superseded by CFSR, ERA5 (Hersbach et al. 2018), and MERRA-2 (Gelaro et al. 2017), respectively. Reanalyses vary in terms of temporal range and horizontal resolution. Thus to eliminate differences due to contrasting resolutions, all reanalyses and observations were re-gridded to a  $1^\circ \times 1^\circ$  horizontal grid for 1979–2013. Note that some products had a resolution higher than  $1^\circ \times 1^\circ$  resolution, so the regridding operation induced additional errors for the comparison.

The reanalyses studied here use different models and assimilation methods, which can lead to differences in the datasets

(Bao and Zhang 2013; Kang et al. 2010; Ma et al. 2009; Simmons et al. 2004; Wang and Zeng 2012; You et al. 2017). Thus, the surface pressure and its trends over the TP may vary across the different reanalyses. To determine how well the reanalyses perform over the TP, surface pressure fields from each reanalysis are compared with the observed monthly surface pressure from the 71 stations.

## 2.2 Observed elevation and model elevation

To explain differences between observations and multiple reanalyses, a topographical analysis is performed using the statistical methods followed by the previous papers (You et al. 2008b, 2013b). The observed elevation of each surface station is provided by NMIC/CMA, and model elevations of each reanalysis (NCEP1, NCEP2, ERA-Interim, MERRA and JRA55) can be obtained from its respective website (Dee et al. 2011; Kalnay et al. 1996; Kanamitsu et al. 2002; Kistler et al. 2001; Kobayashi et al. 2015; Rienecker et al. 2011). All reanalyses are compared at the observations locations. For this, we spatially interpolate all the reanalyses to the exact horizontal position (and elevation) of the 71 surface stations and compare the trends and climatology at the 71 stations rather than the grid points. We interpolate the reanalysis data from the surrounding grid points to the site's location using bilinear interpolation, and transform the grid surface pressure to the observation site's altitude using the hydrostatic equation as in You et al. (2017). The pressure from each reanalysis is corrected to the observed station height assuming a linear lapse rate.

## 2.3 Elevation correction methods

The elevation correction at each station is described by

$$P_2 = P_1 \left[ 1 - \frac{\Gamma(z_2 - z_1)}{T_1} \right]^{\frac{g}{R_d \Gamma}} \quad (1)$$

**Table 1** Summary of the observations and multiple reanalyses used in this study

Name	Organization	Temporal resolution	Horizontal resolution	Assimilation methods	Sources	References
NCEP1	NCEP/NCAR	1948-present	$2.5^\circ \times 2.5^\circ$	3D-VAR	<a href="http://www.esrl.noaa.gov">http://www.esrl.noaa.gov</a>	Kalnay et al. (1996)
NCEP2	NCEP/DOE	1979-present	$2.5^\circ \times 2.5^\circ$	3D-VAR	<a href="http://www.esrl.noaa.gov">http://www.esrl.noaa.gov</a>	Kanamitsu et al. (2002)
ERA-Interim	ECMWF	1979-present	$0.5^\circ \times 0.5^\circ$	4D-VAR	<a href="http://www.ecmwf.int">http://www.ecmwf.int</a>	Dee et al. (2011)
MERRA	NASA GMAO	1979-present	$0.5^\circ \times 0.5^\circ$	3D-VAR, with incremental update	<a href="http://disc.sci.gsfc.nasa.gov">http://disc.sci.gsfc.nasa.gov</a>	Rienecker et al. (2011)
JRA55	JMA	1958-present	$1.25^\circ \times 1.25^\circ$	4D-VAR	<a href="http://jra.kishou.go.jp">http://jra.kishou.go.jp</a>	Kobayashi et al. (2015)

where  $P_2$  and  $P_1$  are the corrected and original reanalysis surface pressures,  $\Gamma$  is the vertical temperature lapse rate,  $z_2$  and  $z_1$  are the model and station elevations,  $T_1$  is the surface air temperature of each reanalysis dataset horizontally interpolated into the observation locations,  $R_d$  is the gas constant for dry air and  $g$  is the acceleration due to gravity. To calculate the  $\Gamma$ , the temperature profiles from sounding data and multiple reanalyses dataset over the TP on an annual and seasonal basis are plotted (Fig. 2). Results indicate that the temperature profiles from the reanalyses are consistent with the observed profiles at the sounding stations over the TP. This suggests that the temperature from the reanalyses can be used to calculate the  $\Gamma$ . The detailed method is shown as follows: First, the pressure level of the lowest layer above the ground is denoted as  $P_1$ , and 300 hPa pressure level is denoted as  $P_2$ . Meanwhile, both temperature ( $T$ ) and geopotential height data ( $H$ ) between level  $P_1$  and  $P_2$  are extracted, respectively. The  $\Gamma$  is calculated by linear regression based the following formula:

$$T = \Gamma H + b \tag{2}$$

Afterwards, the regression coefficient  $\Gamma$  of each station in each year is calculated. The annual and seasonal  $\Gamma$  from multiple reanalyses is summarized in Table 2.

To assess the success of this correction, the root-mean-square error (RMSE) is calculated after correction as:

$$RMSE = \sqrt{\frac{1}{n} \sum_{i=1}^{i=n} (P - P_{obs})^2} \tag{3}$$

**Table 2** Temperature lapse rate from multiple reanalyses datasets over the Tibetan Plateau on an annual and seasonal basis, and the unit is °C/100 m

	Annual	Spring	Summer	Autumn	Winter
NCEP1	-0.66	-0.70	-0.64	-0.64	-0.65
NCEP2	-0.68	-0.73	-0.64	-0.67	-0.69
ERA-Interim	-0.68	-0.73	-0.62	-0.67	-0.72
MERRA	-0.69	-0.74	-0.62	-0.68	-0.73
JRA55	-0.67	-0.73	-0.62	-0.66	-0.69

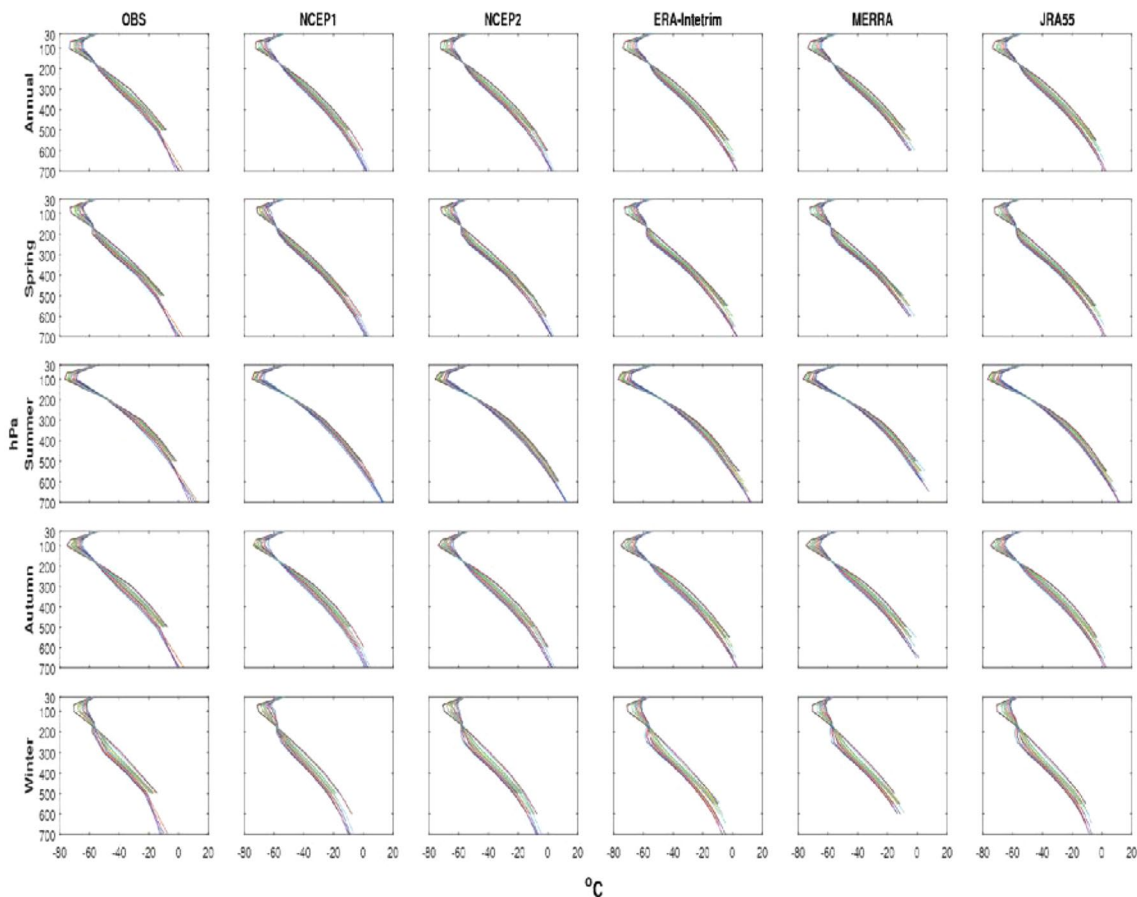


**Fig. 2** Temperature profile from 13 sounding stations and multiple reanalyses over the Tibetan Plateau on an annual and seasonal basis. Each curve within a single panel represents temperature profile from each sounding station and reanalysis

where  $P$  represents corrected surface pressure of each reanalysis in turn,  $P_{obs}$  is the corresponding station observation and  $N$  is the number of station sites.

## 2.4 Diagnostic equation

To investigate the possible mechanism of surface pressure anomalies and long-term trend, the diagnostic equation is performed based on monthly products from ERA-Interim reanalysis (Dee et al. 2011). Based on equation of static equilibrium, low-level geopotential height can be calculated from Eq. (4):

$$z_1 = z_2 - R_d \int_{p_2}^{p_1} \frac{T_v}{g} d \ln p \quad (4)$$

where  $z_1$  and  $z_2$  are 600 hPa and 100 hPa geopotential height, respectively.

Virtual temperature ( $T_v$ ) is given as:

$$T_v = (1 + 0.608q)T, \quad (5)$$

Interannual anomaly of each variable during 1979–2013 is:

$$\Delta A = A - \bar{A} \quad (6)$$

where  $\bar{A}$  is the climate mean states of a variable,  $\Delta A$  is the deviation or anomaly of a variable from climate mean status.

Based on Eq. (6), the interannual anomaly form of Eq. (4) is:

$$\Delta z_1 = \Delta z_2 - R_d \int_{p_2}^{p_1} \frac{\Delta T_v}{gP} dp \quad (7)$$

where  $\Delta z_1$  and  $\Delta z_2$  is interannual anomaly of  $z_1$  and  $z_2$ , respectively.  $\Delta T_v$  is the interannual anomaly of virtual temperature. Equation (7) indicates that the interannual anomaly of  $z_1$  depends on both the interannual anomaly of  $z_2$  and the atmospheric column temperature. Furthermore, the anomaly of  $z_1$  varies in-phase with the anomaly of  $z_2$ , but it has the opposite phase with variation from the anomaly of atmospheric column temperature.

Moreover, atmospheric column temperature is closely associated with atmosphere diabatic heating. The interannual anomaly of diabatic heating  $\Delta Q$  is balanced by the interannual anomalies of latent heat release  $\Delta LH$ , surface sensible heat  $\Delta SH$ , and net atmospheric radiation  $\Delta RC$ .

$$\Delta Q = \Delta LH + \Delta RC + \Delta SH \quad (8)$$

Latent heat  $LH$  can be calculated from precipitation:

$$LH = L_w \rho_w P \quad (9)$$

Net atmospheric radiation  $RC$  can be calculated by the difference from net radiation on the top of atmosphere ( $Rn_{toa}$ ) and net radiation on the surface ground ( $Rn_{sfc}$ ).

$$RC = Rn_{toa} - Rn_{sfc} \quad (10)$$

Finally, trends and significance are estimated using the Mann–Kendall test and Sen's slope estimates (Sen 1968). All time series are calculated at monthly resolution. A trend is considered to be statistically significant if it is significant at the 5% level.

## 3 Results

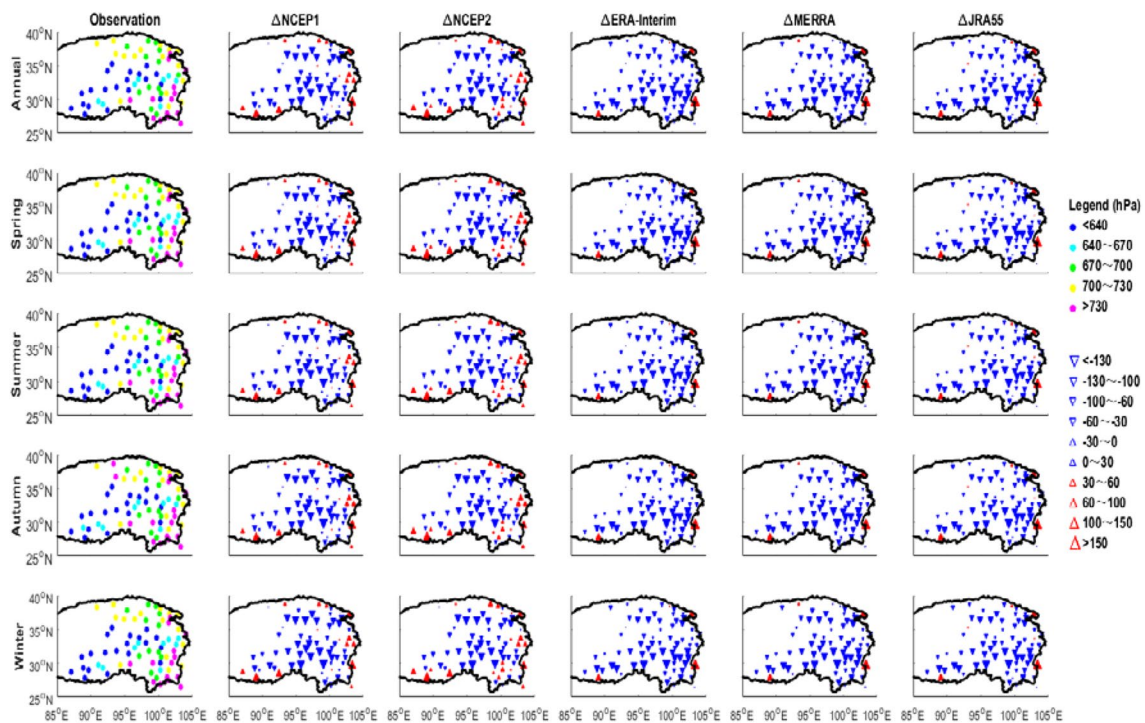
### 3.1 Climatology and variability of surface pressure over the TP

Table 3 summarizes annual and seasonal means and relative bias of surface pressure from both station observations and the five reanalyses (NCEP1, NCEP2, ERA-Interim, MERRA and JRA55) at monthly resolution during 1979–2013. Using station data, the highest/lowest surface pressures occur in autumn/winter. All the reanalyses underestimate the observations with the relative error between 3 and 6%. NCEP2 is closest to the observations and MERRA appears to have the largest differences. The spatial distribution of mean absolute biases (reanalysis minus observation) of surface pressure is shown on an annual and seasonal basis in Fig. 3. All reanalyses underestimate station pressure, which is consistent with the previous study during 2002–2004 (Wang and Zeng 2012). The largest absolute biases occur in the south of the plateau and in areas such as the Sichuan basin, but there are also patches of large negative bias in the north-west of the plateau. It is striking that all five of the reanalyses show similar patterns, reaching over 100 hPa in the worst locations

**Table 3** Annual and seasonal mean and relative bias of surface pressure from station observations and multiple reanalyses (NCEP1, NCEP2, ERA-Interim, MERRA and JRA55) over the Tibetan Plateau during 1979–2013

	Annual	Spring	Summer	Autumn	Winter
Mean (hPa)					
Observation	682.4	681.2	683.0	685.2	680.3
NCEP1	652.4	651.3	653.8	655.1	649.5
NCEP2	658.8	657.7	660.1	661.5	656.0
ERA-Interim	644.8	643.7	646.1	647.5	641.9
MERRA	643.4	642.4	644.9	646.0	640.4
JRA55	645.8	644.7	647.4	648.5	642.6
Relative bias (%)					
NCEP1	− 4.4%	− 4.4%	− 4.3%	− 4.4%	− 4.5%
NCEP2	− 3.5%	− 3.5%	− 3.4%	− 3.5%	− 3.6%
ERA-Interim	− 5.5%	− 5.5%	− 5.4%	− 5.5%	− 5.6%
MERRA	− 5.7%	− 5.7%	− 5.6%	− 5.7%	− 5.9%
JRA55	− 5.4%	− 5.4%	− 5.2%	− 5.4%	− 5.5%

The relative bias is defined as  $\frac{\text{Reanalysis} - \text{Observation}}{\text{Observation}} \times 100\%$



**Fig. 3** Spatial distribution of climatological surface pressure (top left) and difference ( $\Delta$ ) between observation and five reanalyses (NCEP1, NCEP2, ERA-Interim, MERRA and JRA55) before correction con-

sidering the elevation difference over the Tibetan Plateau on an annual and seasonal basis. The unit is hPa

which tend to occur in two latitudinal bands around 30°N and 36°N.

### 3.2 Corrections of surface pressure biases from reanalyses over the TP

All reanalyses underestimate the observed elevation, and much of the difference between observed pressure and reanalysis data may be explained by topographical errors. In most cases, elevation differences (model minus surface station elevation,  $\Delta H$ ) are positive because surface stations are situated in flat areas and valley bottoms which tend to be lower than the reanalysis model topography (You et al. 2013b). Stations over the TP are predominantly in lower mountain valleys on the southern and eastern parts of the plateau, surrounded by higher peaks (where people live). This would explain a general underestimation of surface pressure in the reanalyses. The different spatial resolution between stations (points) and reanalysis grids, coupled with intrinsic topographic bias, can lead to large elevation differences and in part this elevation difference causes the differences in the surface pressure. The underestimation of surface pressure in all reanalyses is mainly explained by the overestimation of the elevation in the model. This is consistent with previous studies (Ma et al. 2008, 2009; You et al. 2008b, 2013b) which found a cold bias of NCEP/NCAR and

ERA-40 to be mainly a result of differences in topographical height, and secondly due to station aspect and slope gradient.

Because much of the surface pressure bias between observations and reanalyses is explained by elevation differences, it is vital to remove this (Kang et al. 2010; Ma et al. 2008, 2009; Song et al. 2016; Xie et al. 2014; You et al. 2013b, 2017; Zhao et al. 2008). Thus, the interpolated surface pressure was corrected for each reanalysis separately using the topographic correction. The spatial distribution of mean absolute bias (corrected reanalyses minus observation) is shown in Fig. 4. The percentage of improvement after corrections is summarized in the bottom rows of Table 4. Dramatic improvements are achieved through elevation correction and differences of all reanalysis datasets are reduced by more than 90%. The best results are ERA-Interim and MERRA whose difference is reduced by more than 95%, closely followed by JRA55. The success of elevation correction for temperature showed seasonal and regional dependency (Zhao et al. 2008), and is slightly better in summer than in winter. This is unsurprising since the vertical structure of the atmosphere is typically more well-mixed and uniform in summer, and inversions are less frequent (which would invalidate a simple correction) (Pepin et al. 2011; You et al. 2017). For surface pressure, the effects of the correction also show seasonal dependence, and the remaining bias after correction does show some spatial variance.

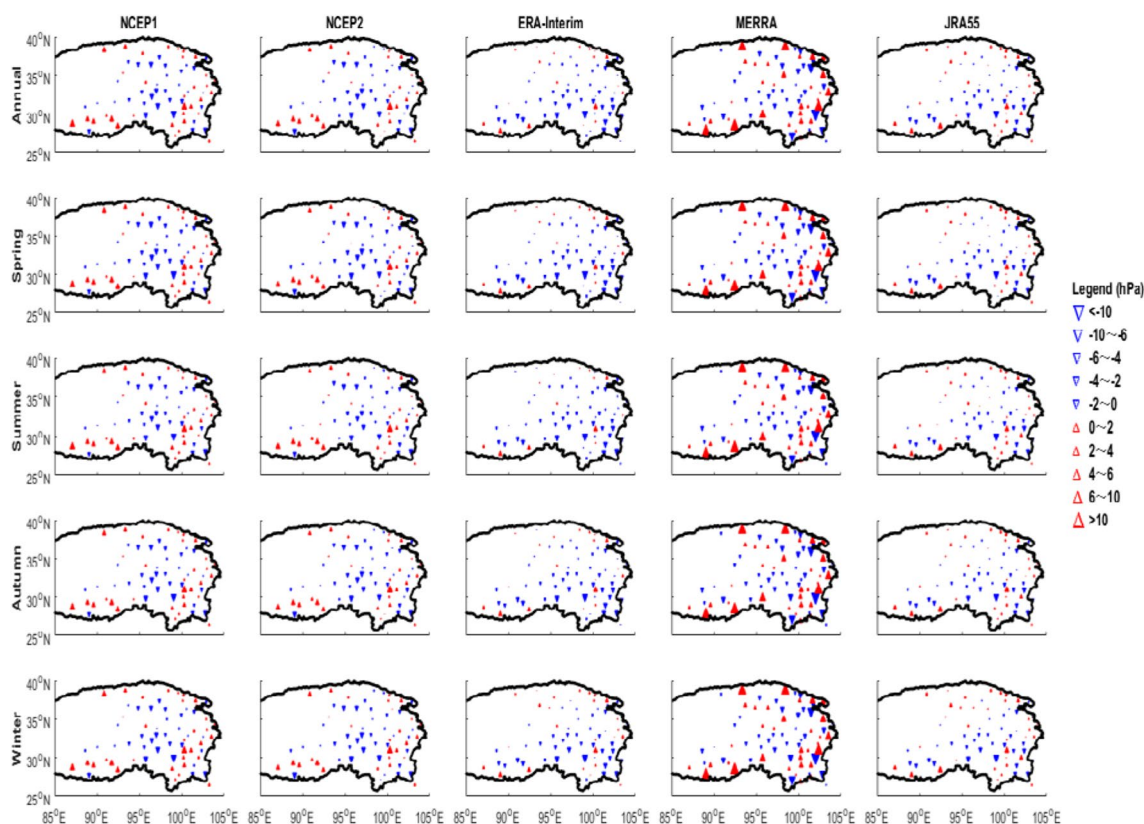


**Fig. 4** Spatial distribution of mean absolute biases (corrected reanalysis minus observation) of surface pressure over the Tibetan Plateau on an annual (top row) and seasonal basis (other rows). The unit is hPa

**Table 4** Root mean square error of reanalyses surface pressure (reanalyses vs observations) for horizontal bilinear interpolation and correction considering the elevation difference on an annual and seasonal basis

	Annual	Spring	Summer	Autumn	Winter
Horizontal bilinear interpolation					
NCEP1	57.5	57.4	55.9	57.6	59.1
NCEP2	54.7	54.6	53.1	54.8	56.2
ERA Interim	56.2	56.1	54.9	56.3	57.6
MERRA	57.8	57.6	56.3	58.0	59.3
JRA55	55.6	55.5	54.1	55.8	57.2
Interpolation considering elevation difference					
NCEP1	3.7	3.7	3.3	3.7	4.2
NCEP2	3.0	3.0	2.9	3.0	3.3
ERA-Interim	2.2	2.2	2.1	2.2	2.4
MERRA	2.2	2.2	2.1	2.2	2.4
JRA55	2.6	2.5	2.5	2.5	2.7
Percentage of improvement after correction					
NCEP1	93.6%	93.6%	94.1%	93.7%	92.8%
NCEP2	94.5%	94.5%	94.5%	94.5%	94.1%
ERA-Interim	96.2%	96.1%	96.2%	96.1%	96.0%
MERRA	96.2%	96.2%	96.3%	96.2%	96.0%
JRA55	95.4%	95.4%	95.4%	95.4%	95.2%

The percentage reduction in bias after correction is listed

The bias for MERRA (which remains relatively large) is more than 30 hPa in southern parts of the TP but less than 4 hPa in central areas. Most regions show relatively small biases between  $-5$  and 10 hPa for NCEP1, NCEP2, ERA-Interim and JRA55. The complexity of the terrain, especially towards the southern edge of the plateau, is probably responsible for some of the remaining bias, consistent with past studies on temperature (Zhao et al. 2008).

### 3.3 Trend of surface pressure after correction over the TP

Figures 5 and 6 show the regional anomaly and spatial trends of surface pressure from observations and reanalyses after correction considering the elevation difference over the TP on an annual and seasonal basis. Table 5 summarizes the annual and seasonal means and trends of surface pressure from observation and multiple reanalyses after elevation bias correction. On an annual basis, mean regional surface pressure series from both observations and reanalyses increase slowly until the mid-2000s but then show a significant decrease afterwards (Fig. 5). It is also clear that all reanalyses are strongly correlated with the station data, indicating that they can clearly reproduce decadal variation in surface



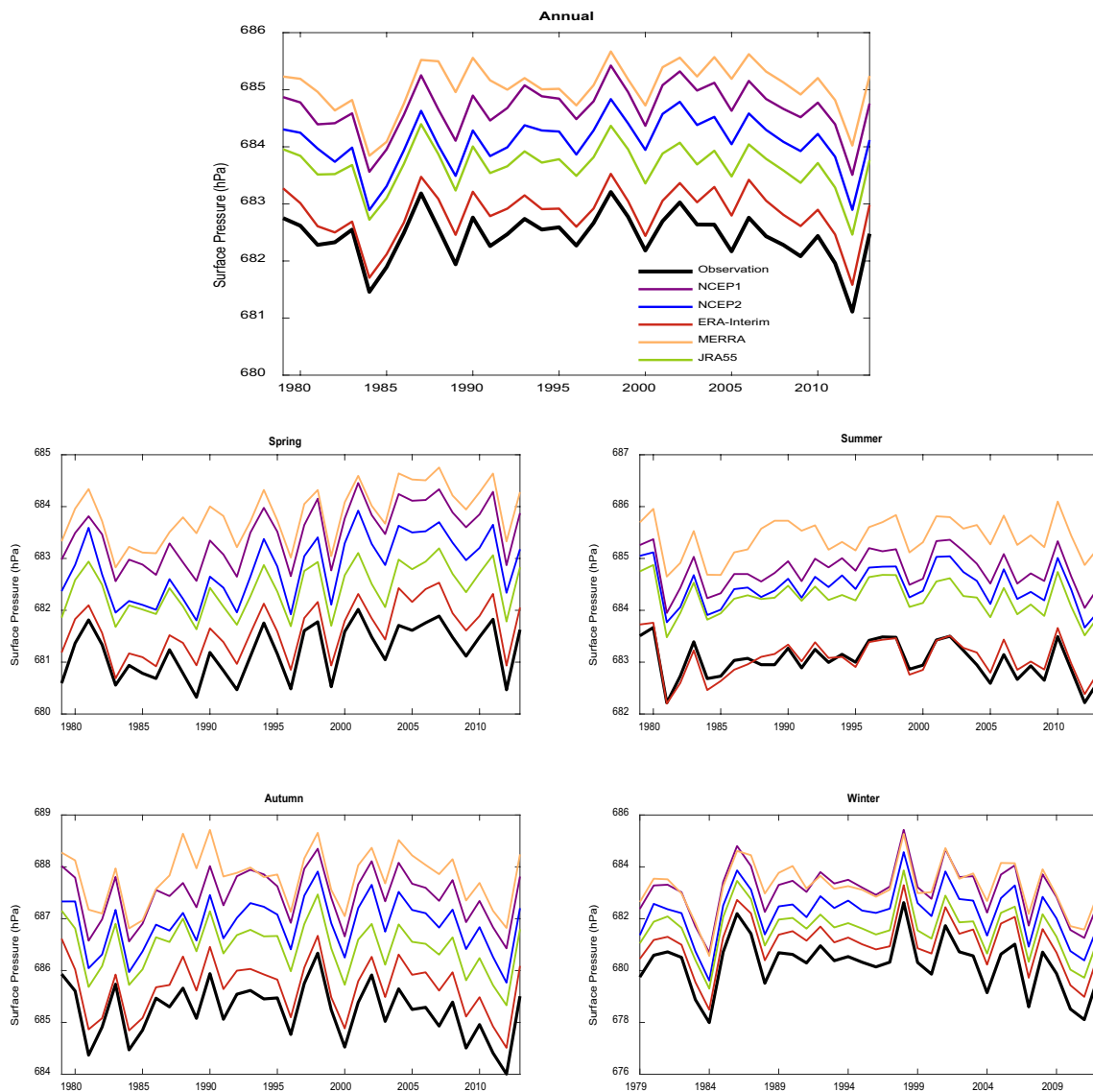


**Fig. 5** Regional anomaly of surface pressure from observations and each reanalysis (NCEP1, NCEP2, ERA-Interim, MERRA and JRA55) after horizontal bilinear interpolation and corrected by alti-

tude bias over the Tibetan Plateau during 1979–2013 on an annual (top panel) and seasonal basis (other four panels)

pressure. Over the whole period, the trends of surface pressure are insignificant from all sources. Examining spatial patterns in more detail, the majority of individual stations shows a decrease in surface pressure. During 1979–2013, it is clear most stations in the central/northern regions show significant negative trends on an annual basis (Fig. 6, top left panel). Stations in the central and northern TP tend to have larger trend magnitudes, which correspond with downward trends in total cloud cover and surface relative humidity in the region (You et al. 2015b). However, reanalyses tend to show increases in pressure over the same period, particularly NCEP1 and MERRA. On a seasonal basis, the trends over the whole period from observations and reanalyses also show large differences. The maps show areas of significant

trend change, and both observations and reanalyses show largest increases in spring. The other seasons have smaller trend values which in most regions are insignificant. As was the case for annual trends, the observations again show more negative trends in general than reanalyses in most seasons.

### 3.4 Possible mechanism influencing surface pressure over the TP

To investigate possible mechanisms that influence surface pressure over the TP, especially in spring, an atmospheric diagnosis is performed based on ERA-Interim reanalysis. Figure 7 shows the time series of surface pressure anomalies, 100 hPa and 600 hPa geopotential height, and column

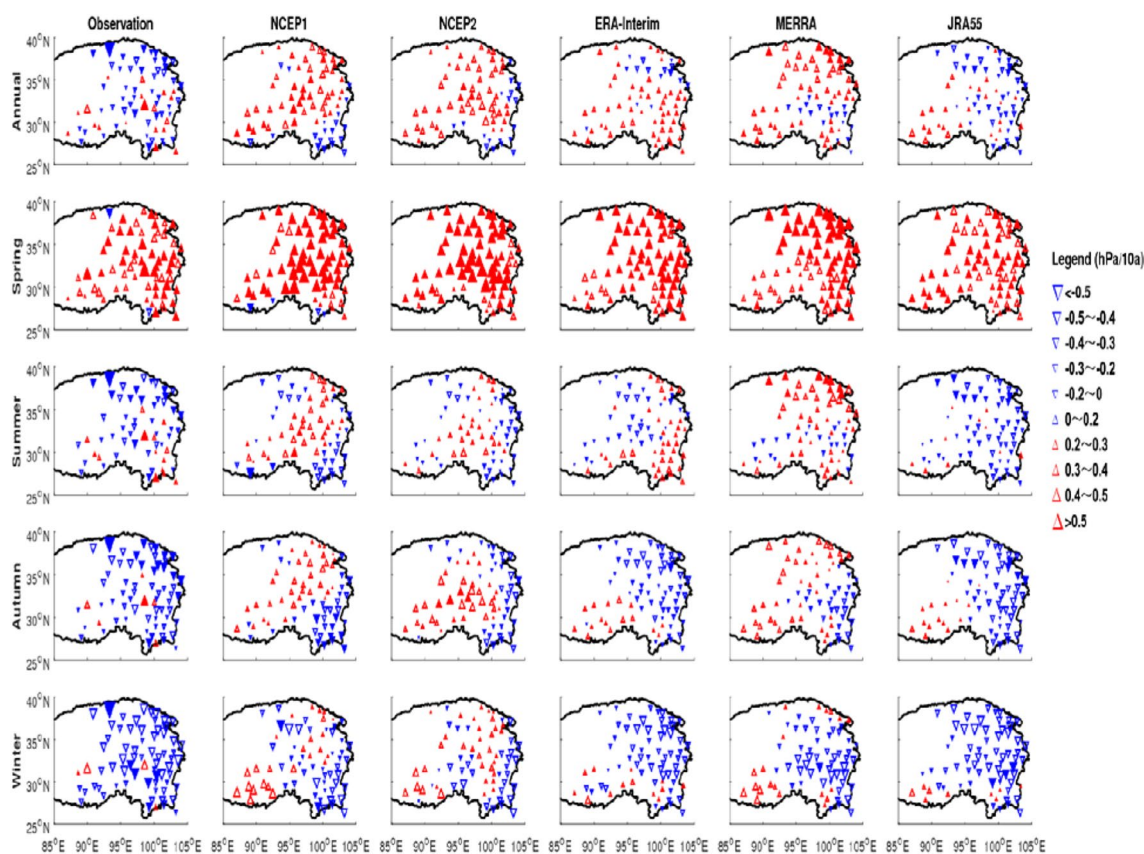


**Fig. 6** Spatial trends of surface pressure from observations (top left) and the five reanalyses (NCEP1, NCEP2, ERA-Interim, MERRA and JRA55) after correction considering the elevation difference over the

Tibetan Plateau during 1979–2013 on an annual and seasonal basis. The unit is hPa/decade. The solid/hollow triangles are the stations with trend passed/failed the significant test

**Table 5** Annual and seasonal mean and trend of surface pressure from station observations and multiple reanalyses (NCEP1, NCEP2, ERA-Interim, MERRA and JRA55) after correction considering the elevation difference over the Tibetan Plateau during 1979–2013

	Annual	Spring	Summer	Autumn	Winter
<b>Mean (hPa)</b>					
Observation	682.4	681.2	683.0	685.2	680.3
NCEP1	684.7	683.5	684.8	687.5	683.1
NCEP2	684.1	682.8	684.5	686.9	682.2
ERA-Interim	682.8	681.6	683.1	685.7	681.0
MERRA	685.1	683.9	685.4	687.8	683.2
JRA55	683.7	682.4	684.2	686.5	681.6
<b>Trend (hPa/decade)</b>					
1979–2013					
Observation	-0.04	0.21	-0.06	-0.13	-0.23
NCEP1	0.06	0.33	0.02	-0.02	-0.05
NCEP2	0.06	0.35	-0.01	0.01	-0.02
ERA interim	0.02	0.27	0.02	-0.03	-0.15
MERRA	0.07	0.30	0.05	0.01	-0.11
JRA55	-0.02	0.23	-0.06	-0.11	-0.18

temperature over the TP during 1979–2013. Table 6 summarizes the correlation coefficients among these variables in spring. It is clear that the surface pressure over the TP is positively correlated with the 100 hPa and 600 hPa geopotential height, with correlation coefficients of 0.4 and 0.97, respectively. Thus, the changes of surface pressure over the TP can be inferred from the 600 hPa geopotential height. Meanwhile, the surface pressure over the TP has similar interannual variabilities with 100 hPa and 600 hPa geopotential height, indicating the quasi-barotropic atmospheric structure over the TP.

From Eqs. (4–8) in the methods, the changes of 600 hPa geopotential height are determined by 100 hPa geopotential height and atmospheric column temperature, then indirectly influence the surface pressure over the TP. Moreover, the atmospheric column temperature is influenced by diabatic heating, which is balanced by latent heat, surface sensible heat and atmospheric net radiation, respectively. Figures 8 and 9 show the time series and spatial trends of standardized column temperature, diabatic heating, latent heat, surface sensible heat, and net atmospheric radiation over the TP during 1979–2013 on an annual and seasonal

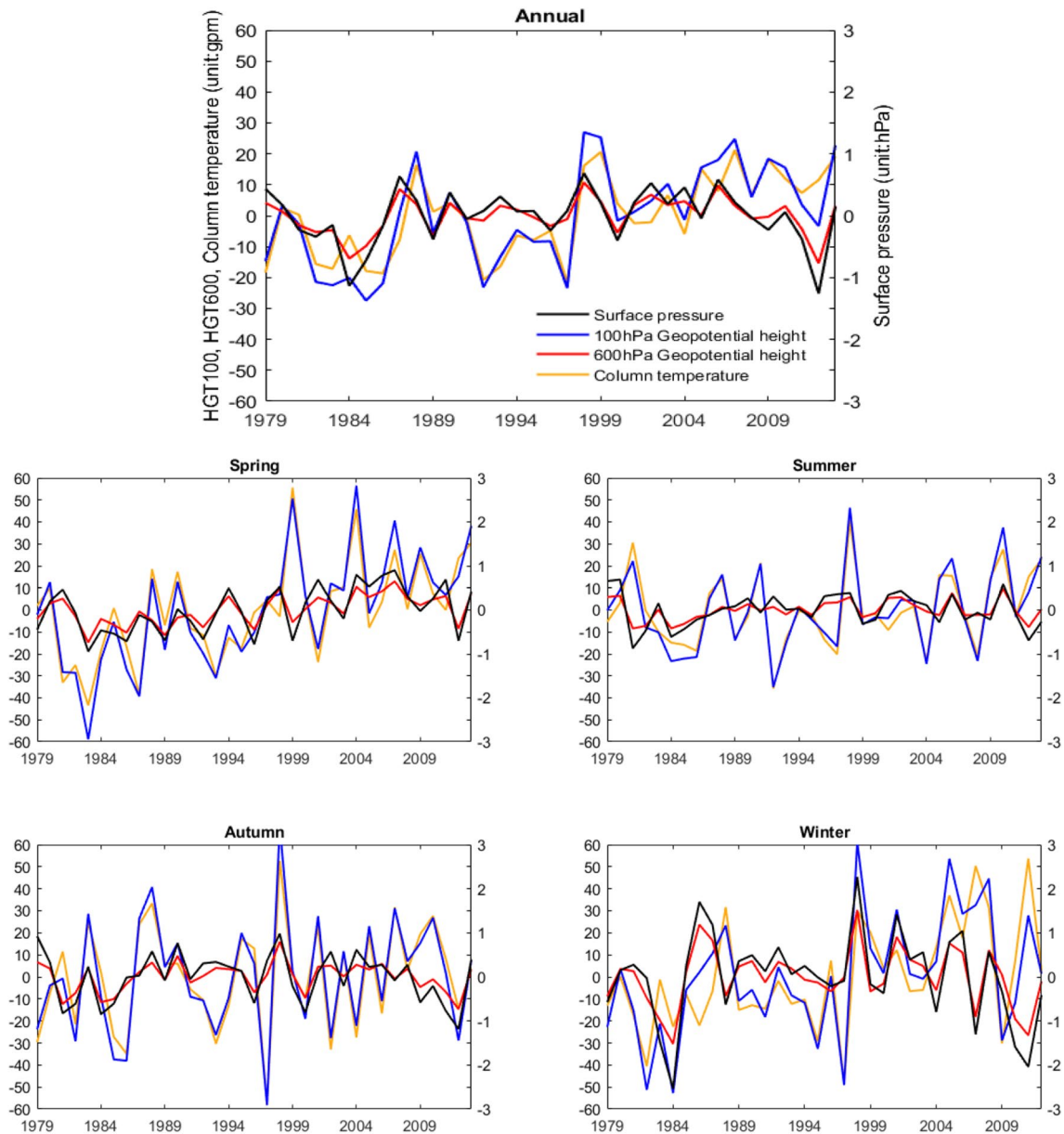


**Fig. 7** Time series of surface pressure anomalies (black line, hPa), 100 hPa geopotential height (blue line, gpm), 600 hPa geopotential height (red line, gpm), and column temperature (yellow line, °C) over

the Tibetan Plateau during 1979–2013 on an annual and seasonal basis based on ERA-Interim dataset

**Table 6** Correlation coefficients among surface pressure, 100 hPa geopotential height, 600 hPa geopotential height, and column air temperature based on ERA-Interim dataset over the Tibetan Plateau in spring during 1979–2013

Correlation coefficient	Surface pressure	100 hPa geopotential height	600 hPa geopotential height	Column temperature
Surface pressure	1	–	–	–
100 hPa geopotential height	0.40**	1	–	–
600 hPa geopotential height	0.97**	0.50**	1	–
Column temperature	0.16	0.96**	0.26	1

The single and double asterisks indicate the value passed the 0.1 and 0.05 significant level, respectively

basis based on ERA-Interim reanalysis. Their correlation coefficients are summarized in Table 7. The column temperature has negative correlations with both surface

sensible heat and net atmospheric radiation, and positive correlations with diabatic heating and latent heat, and all the correlation coefficients pass the significance test

**Fig. 8** Time series of standardized column air temperature (black solid line), diabatic heating (black dashed line), air latent heat (red solid line), surface sensible heat (blue solid line), and net atmospheric radiation (yellow line) over the Tibetan Plateau during 1979–2013 on an annual and seasonal basis based on ERA-Interim dataset. Both net atmospheric radiation and diabatic heating contain the period of 1983–2007, which were obtained from the NASA Langley Research Center Atmospheric Sciences Data Center NASA/GEWEX SRB Project (<https://gewex-srb.larc.nasa.gov/>)

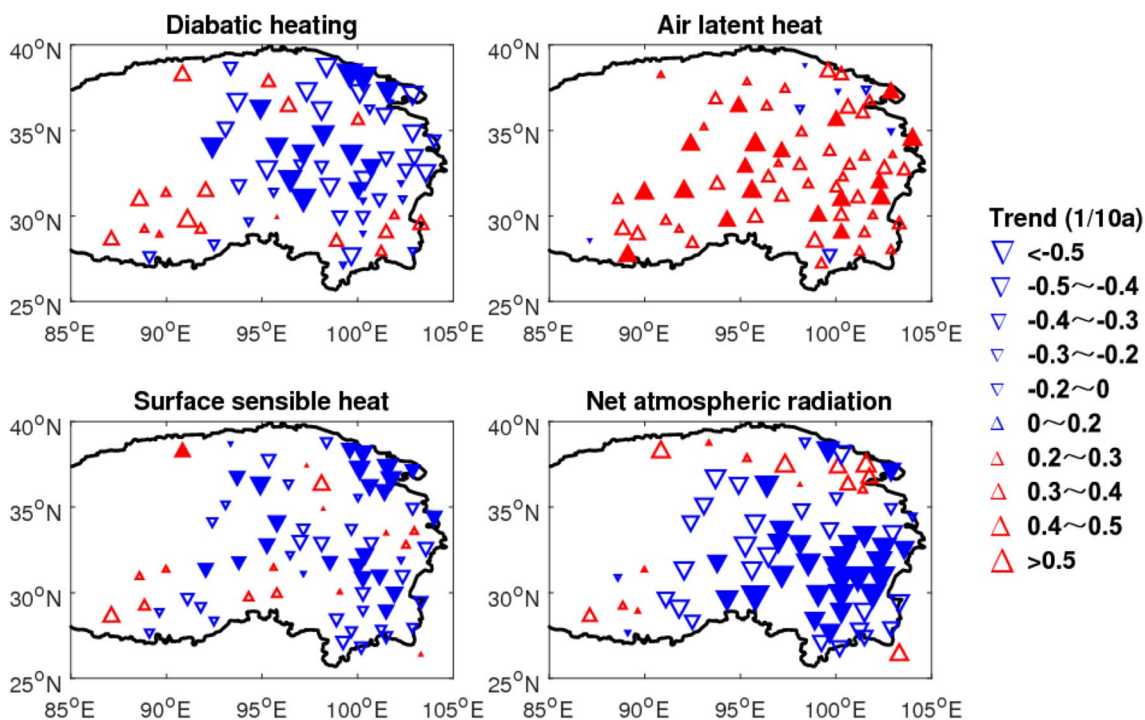
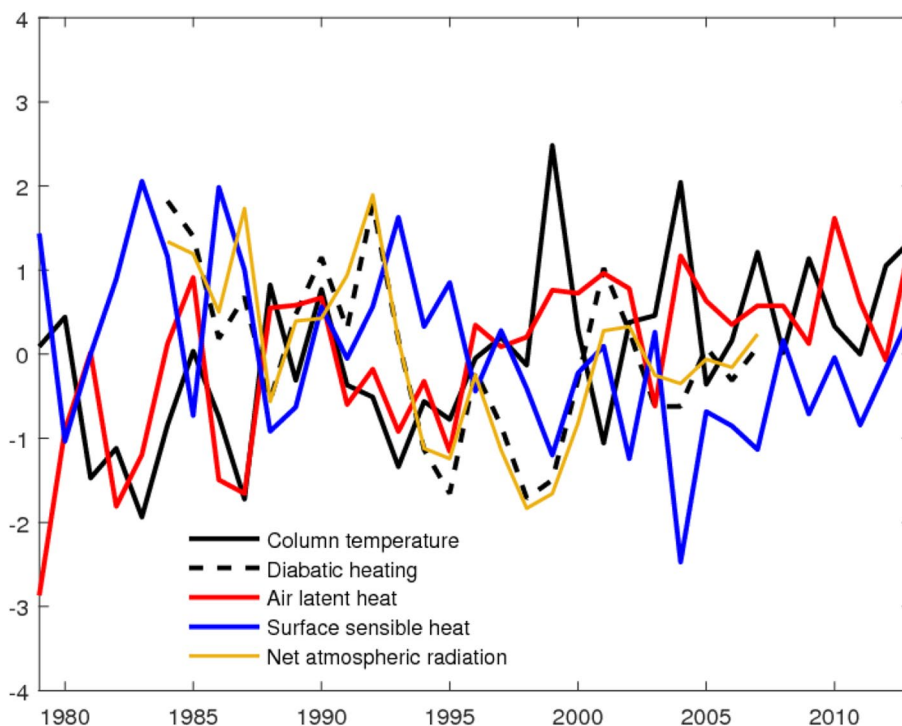


**Fig. 9** Spatial trends of diabatic heating, air latent heat, surface sensible heat and net atmospheric radiation over the Tibetan Plateau in spring. The solid/hollow triangles are the stations with trend passed/failed the significance test

(Table 7). In Fig. 9, it is clear that decreasing sensible heat increases the heat flux transformation from ground to the bottom air, and increasing latent heat leads to the endothermic increases, as well as the decreasing net atmospheric radiation results to the energy transferring from atmosphere to surface. These changes contribute to the decreasing diabatic heating, causing the increase of atmospheric column temperature, which is consistent with the increasing column temperature over the TP (Fig. 10). Thus, this suggests that the significant increase of both 100 hPa geopotential height and column temperature over the TP mainly accounts for the significant increase of surface pressure over the TP.

**Table 7** Correlation coefficients between column temperature and diabatic heating, air latent heat, surface sensible heat, as well as net atmospheric radiation based on ERA-Interim dataset over the Tibetan Plateau in spring during 1979–2013

	Diabatic heating	Air latent heat	Surface sensible heat	Net atmospheric radiation
Correlation coefficient	-0.36*	0.51**	-0.67**	0.43**

The single and double asterisks indicate the value passed the 0.1 and 0.05 significant level, respectively

## 4 Discussion and conclusions

In this study, the variability and reliability of surface pressure over the TP are analyzed from station observations and multiple reanalyses during 1979–2013. This is the first time that such analyses have been performed at high elevations and this is an important finding, given that mountain station pressure can be regarded as an indicator of climate change (Toumi et al. 1999). This suggests that the vertical expansion/warming of the atmosphere at high elevations will not necessarily lead to increased pressure at high elevation stations. The physical relationship between the surface temperature and pressure reflects the changing nature of the seasonal snow cover (land surface property) and cloud in the region (You et al. 2017). Meanwhile, the finding that all reanalyses underestimate surface pressure over the TP is consistent with other studies. Recent work in East Antarctica shows reanalyses explain more than 87% of the average variance of surface pressure shown by observations during 2005–2008 (Xie et al. 2014). Despite discrepancies between observations and reanalyses, inter-annual correlations between the two were high. Similar results were also shown over the Southern Ocean and Antarctica (Hines et al. 2000) since the 1980s. Thus our finding that surface pressure from reanalyses (NCEP1, NCEP2, ERA-Interim, MERRA and JRA55) over the TP is broadly similar to surface pressure from observations

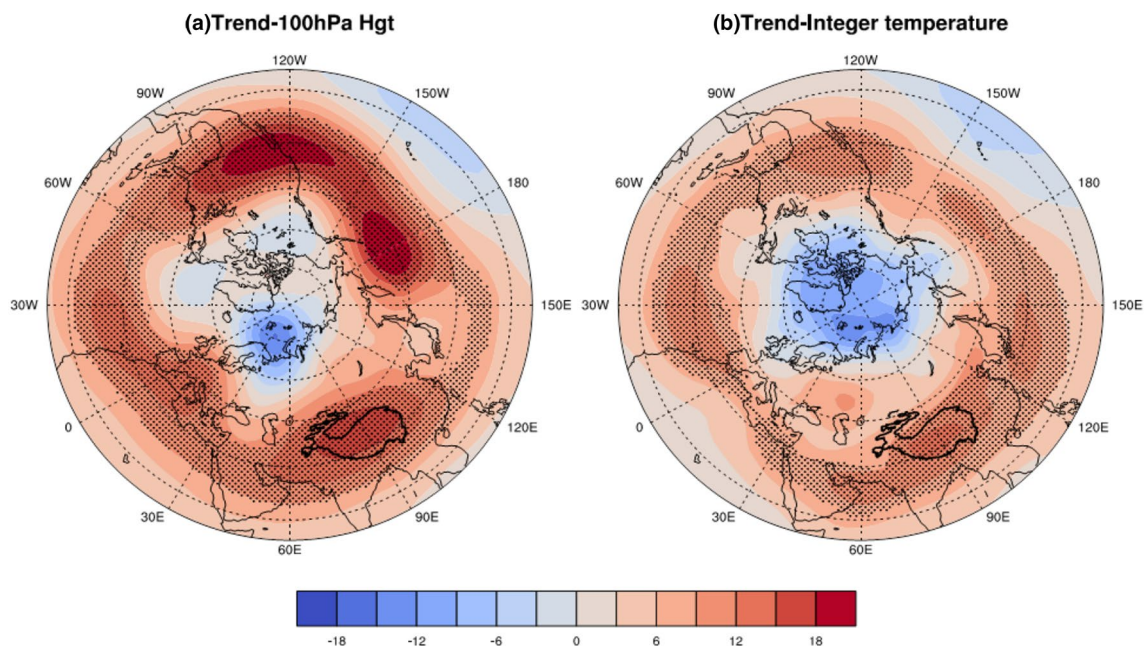


**Fig. 10** Spatial trends of **a** 100 hPa geopotential height (gpm/decade) and **b** column temperature (°C/decade). The shaded area represents where the trend passed the significant test

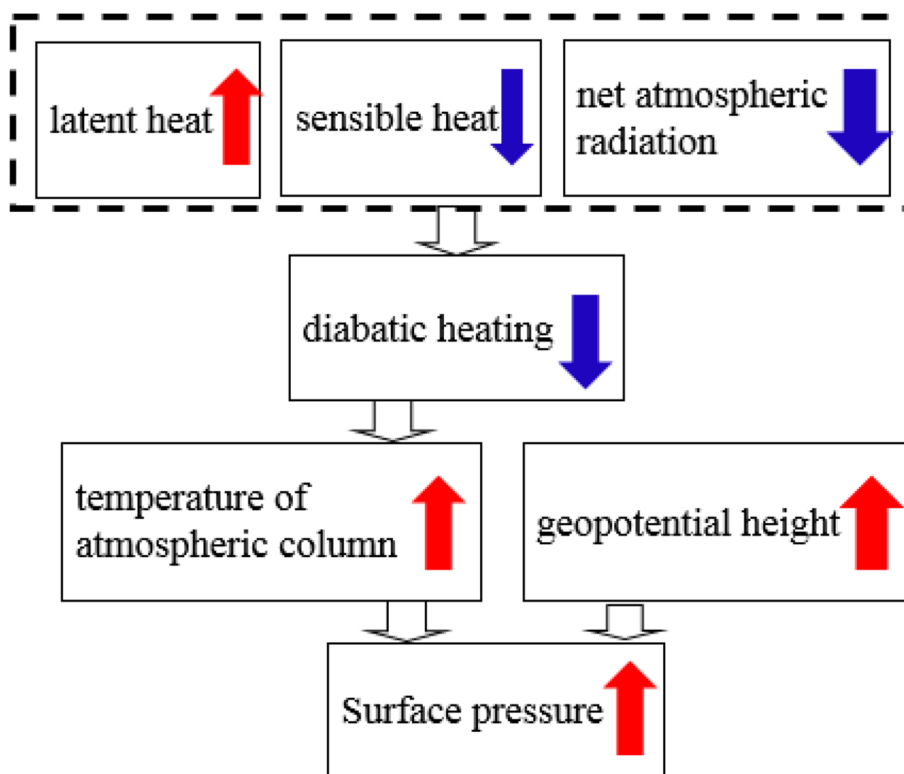
and that reanalyses can capture the decadal variability of pressure is supported by analyses elsewhere.

Analysis of pressure trends in this study reveals a significant decrease of surface pressure after the mid-2000s in both observations and all reanalyses. In this study, it is found that the increases in both 100 hPa geopotential height and column temperature over the TP result in increases in 600 hPa geopotential height, which likely account for the significant increase of surface pressure in spring over the TP (Fig. 11). However, there is little variation in temperature lapse rate with season, with the highest temperature lapse rate in spring. The surface pressure change is not related to the change of temperature lapse rate, but is associated with the altitude difference with larger trend magnitude. A scaling of the vertical equation of motion shows on monthly time scales the vertical motion is negligible. The elevation biases extrapolated to the stations is accurately given, and the effect of vertical interpolation will be helpful through using hydrostatic equation. Thus, pressure increase is most evident in spring, which doesn't depend on the value of the temperature lapse rate but on the thermal condition change over the TP.

There are significant negative correlations between surface pressure bias and elevation bias (reanalysis minus observation) on both an annual and seasonal basis, suggesting that elevation difference is the main reason for the surface pressure biases. This phenomenon has also been revealed for surface air temperature over the TP (You et al.

2013b) and in eastern China (Zhao et al. 2008). Therefore, topographical correction is essential before other analyses are conducted, and most of the bias can be eliminated through topographical correction. ERA-Interim, MERRA and JRA55 perform best after the elevation correction and the percentage of improvement after correction is more than 95%, while NCEP1 and NCEP2 perform the second-best in interpolation considering elevation difference with the percentage of improvement after correction of 94% (Table 4). The better performance of ERA-Interim, MERRA and JRA55 is probably due to the forecast model, the observation handling, operational weather forecasting and assimilation methods (Dee et al. 2011; Rienecker et al. 2011; Simmons et al. 2004). After correction there are still biases in some of the more pronounced basins (e.g. Qaidam basin) and on the southern edges of the plateau where the topography is particularly complex. Most of the surface stations in the TP are located in the central and eastern parts of the TP, and therefore their topographic slope or station orientation could influence the trend magnitudes of pressure over the TP to a certain degree (You et al. 2013b). Future work must therefore go beyond elevational differences and consider topographical factors such as slope aspect, exposure (convexity and concavity) and their influences on explaining remaining bias. This can further reduce uncertainty caused by the complex topography (Moore, 2012; Toumi et al. 1999; Trenberth et al. 1987). Reanalyses can be used to extend surface pressure trend analysis to the western TP where there

**Fig. 11** Possible mechanism influencing surface pressure over the Tibetan Plateau in spring. The upward/downward arrows indicate the positive/negative trends, and the size of arrow is proportional to the magnitude of the trends



are few stations, but it is critical to calibrate the reanalyses against station observations where they exist, which in turn will require a more detailed understanding of topographic factors on model bias (You et al. 2008a, 2013b, 2017). This requires that reanalyses release the observations they used, so that one can verify that the calibration observations are independent from reanalysis.

**Acknowledgements** This study is supported by National Key R&D Program of China (2016YFA0601702) and National Natural Science Foundation of China (41771069). NCEP Reanalysis data are provided by the NOAA/OAR/ESRL PSD, Boulder, Colorado, USA, from their Web site at <https://www.esrl.noaa.gov/psd/>. We are very grateful to the reviewers for their constructive comments and thoughtful suggestions.

## References

- Allan R, Ansell T (2006) A new globally complete monthly historical gridded mean sea level pressure dataset (HadSLP2): 1850–2004. *J Clim* 19(22):5816–5842. <https://doi.org/10.1175/JCLI3937.1>
- Bao X, Zhang F (2013) Evaluation of NCEP–CFSR, NCEP–NCAR, ERA-Interim, and ERA-40 reanalysis datasets against independent sounding observations over the Tibetan Plateau. *J Clim* 26(1):206–214
- Barnett TP, Adam JC, Lettenmaier DP (2005) Potential impacts of a warming climate on water availability in snow-dominated regions. *Nature* 438(7066):303–309. <https://doi.org/10.1038/nature04141>
- Cai D, You Q, Fraedrich K, Guan Y (2017) Spatiotemporal Temperature Variability over the Tibetan Plateau: altitudinal dependence associated with the global warming hiatus. *J Clim* 30:969–984. <https://doi.org/10.1175/jcli-d-16-0343.1>
- Chen TC, Chen JM, Schubert S, Takacs LL (1997) Seasonal variation of global surface pressure and water vapor. *Tellus A* 49:613–621
- Compo GP, Whitaker JS, Sardeshmukh PD (2006) Feasibility of a 100-year reanalysis using only surface pressure data. *Bull Am Meteorol Soc* 87:175–190
- Cullather R, Lynch A (2003) The annual cycle and interannual variability of atmospheric pressure in the vicinity of the North Pole. *Int J Climatol* 23(10):1161–1183
- Cuo L, Zhang Y, Wang Q, Zhang L, Zhou B, Hao Z, Su F (2013) Climate change on the Northern Tibetan Plateau during 1957–2009: spatial patterns and possible mechanisms. *J Clim* 26(1):85–109. <https://doi.org/10.1175/jcli-d-11-00738.1>
- Dee DP et al (2011) The ERA-Interim reanalysis: configuration and performance of the data assimilation system. *Q J R Meteorol Soc* 137(656):553–597. <https://doi.org/10.1002/qj.828>
- Duan AM, Wu GX (2005) Role of the Tibetan Plateau thermal forcing in the summer climate patterns over subtropical Asia. *Clim Dyn* 24(7–8):793–807. <https://doi.org/10.1007/s00382-004-0488-8>
- Duan AM, Wu G, Liu Y, Ma Y, Zhao P (2012) Weather and climate effects of the Tibetan Plateau. *Adv Atmos Sci* 29(5):978–992. <https://doi.org/10.1007/s00376-012-1220-y>
- Fu R, Hu Y, Wright JS, Jiang JH, Dickinson RE, Chen M, Filipiak M, Read WG, Waters JW, Wu DL (2006) Short circuit of water vapor and polluted air to the global stratosphere by convective transport over the Tibetan Plateau. *Proc Natl Acad Sci* 103(15):5664–5669
- Gelaro R et al (2017) The modern-era retrospective analysis for research and applications, Version 2 (MERRA-2). *J Clim* 30(14):5419–5454. <https://doi.org/10.1175/JCLI-D-16-0758.1>
- Gillett NP, Zwiers FW, Weaver AJ, Stott P (2003) Detection of human influence on sea-level pressure. *Nature* 422:292–294
- Hahn DG, Shukla J (1976) An apparent relationship between eurasian snow cover and indian monsoon rainfall. *J Atmos Sci* 33(12):2461–2462. [https://doi.org/10.1175/1520-0469\(1976\)033%3c2461:AARBES%3e2.0.CO;2](https://doi.org/10.1175/1520-0469(1976)033%3c2461:AARBES%3e2.0.CO;2)
- Han W et al (2010) Patterns of Indian Ocean sea-level change in a warming climate. *Nat Geosci* 3(8):546–550
- Hersbach H, de Rosnay P, Bell B, Schepers D, Simmons A, Soci C, Abdalla S, Alonso-Balmaseda M, Balsamo GB (2018) Operational global reanalysis: progress, future directions and synergies with NWP, ERA Report Series 27. ECMWF, Shinfield Park
- Hines KM, Bromwich DH, Marshall GJ (2000) Artificial surface pressure trends in the NCEP–NCAR reanalysis over the Southern Ocean and Antarctica. *J Clim* 13(22):3940–3952
- Ingleby B (2015) Global assimilation of air temperature, humidity, wind and pressure from surface stations. *Q J R Meteorol Soc* 141(687):504–517. <https://doi.org/10.1002/qj.2372>
- Jacques AA, Horel JD, Crosman ET, Vernon FL (2015) Central and Eastern US surface pressure variations derived from the US array network. *Mon Weather Rev* 143(4):1472–1493. <https://doi.org/10.1175/mwr-d-14-00274.1>
- Kalnay E et al (1996) The NCEP/NCAR 40-year reanalysis project. *Bull Am Meteorol Soc* 77(3):437–471
- Kanamitsu M, Ebisuzaki W, Woollen J, Yang SK, Hnilo JJ, Fiorino M, Potter GL (2002) NCEP-DOE AMIP-II reanalysis (R-2). *Bull Am Meteorol Soc* 83(11):1631–1643. <https://doi.org/10.1175/bams-83-11-1631>
- Kang SC, Xu YW, You QL, Flugel WA, Pepin N, Yao TD (2010) Review of climate and cryospheric change in the Tibetan Plateau. *Environ Res Lett* 5(1):015101. <https://doi.org/10.1088/1748-9326/5/1/015101>
- Kistler R et al (2001) The NCEP-NCAR 50-year reanalysis: monthly means CD-ROM and documentation. *Bull Am Meteorol Soc* 82(2):247–267
- Kobayashi S et al (2015) The JRA-55 reanalysis: general specifications and basic characteristics. *J Meteorol Soc Jpn* 93:5–48
- Koppel LL, Bosart LF, Keyser D (2000) A 25-yr climatology of large-amplitude hourly surface pressure changes over the conterminous United States. *Mon Weather Rev* 128(1):51–68
- Liu X, Cheng Z, Yan L, Yin Z-Y (2009) Elevation dependency of recent and future minimum surface air temperature trends in the Tibetan Plateau and its surroundings. *Global Planet Change* 68(3):164–174
- Ma LJ, Zhang TJ, Li QX, Frauenfeld OW, Qin DH (2008) Evaluation of ERA-40, NCEP-1, and NCEP-2 reanalysis air temperatures with ground-based measurements in China. *J Geophys Res Atmos* 113:D15115. <https://doi.org/10.1029/2007jd009549>
- Ma LJ, Zhang T, Frauenfeld OW, Ye BS, Yang DQ, Qin DH (2009) Evaluation of precipitation from the ERA-40, NCEP-1, and NCEP-2 Reanalyses and CMAP-1, CMAP-2, and GPCP-2 with ground-based measurements in China. *J Geophys Res Atmos* 114:D09105
- Mass CF, Madaus LE (2014) Surface pressure observations from smartphones: a potential revolution for high-resolution weather prediction? *Bull Am Meteorol Soc* 95(9):1343–1349
- Moore G (2012) Surface pressure record of Tibetan Plateau warming since the 1870s. *Q J R Meteorol Soc* 138(669):1999–2008
- Pepin NC, Daly C, Lundquist J (2011) The influence of surface versus free-air decoupling on temperature trend patterns in the western United States. *J Geophys Res Atmos* 116:D10109. <https://doi.org/10.1029/2010jd014769>
- Rangwala I, Miller J, Russell G, Xu M (2010) Using a global climate model to evaluate the influences of water vapor, snow cover and atmospheric aerosol on warming in the Tibetan Plateau during the twenty-first century. *Clim Dyn* 34(6):859–872

- Rienecker MM et al (2011) MERRA: NASA's modern-era retrospective analysis for research and applications. *J Clim* 24(14):3624–3648. <https://doi.org/10.1175/jcli-d-11-00015.1>
- Saha K, van den Dool H, Saha S (1994) On the annual cycle in surface pressure on the Tibetan Plateau compared to its surroundings. *J Clim* 7(12):2014–2019
- Sen PK (1968) Estimates of regression coefficient based on Kendall's tau. *J Am Stat Assoc* 63:1379–1389
- Simmons AJ, Jones PD, Bechtold VD, Beljaars ACM, Kallberg PW, Saarinen S, Uppala SM, Viterbo P, Wedi N (2004) Comparison of trends and low-frequency variability in CRU, ERA-40, and NCEP/NCAR analyses of surface air temperature. *J Geophys Res Atmos* 109:D24115. <https://doi.org/10.1029/2004jd005306>
- Song CQ, Ke LH, Richards KS, Gui YZ (2016) Homogenization of surface temperature data in High Mountain Asia through comparison of reanalysis data and station observations. *Int J Climatol* 36:1088–1101
- Toumi R, Hartell N, Bignell K (1999) Mountain station pressure as an indicator of climate change. *Geophys Res Lett* 26(12):1751–1754
- Trenberth KE (1981) Seasonal variations in global sea level pressure and the total mass of the atmosphere. *J Geophys Res Atmos* 86:5236–5246
- Trenberth KE, Christy JR, Olson JG (1987) Global atmospheric mass, surface pressure, and water vapor variations. *J Geophys Res Atmos* 92:14815–14826
- van den Dool HM, Saha S (1993) Seasonal redistribution and conservation of atmospheric mass in a general circulation model. *J Clim* 6(1):22–30. [https://doi.org/10.1175/1520-0442\(1993\)006%3c0022:SRACOA%3e2.0.CO;2](https://doi.org/10.1175/1520-0442(1993)006%3c0022:SRACOA%3e2.0.CO;2)
- Van Wijngaarden W (2005) Examination of trends in hourly surface pressure in Canada during 1953–2003. *Int J Climatol* 25(15):2041–2049
- Wang A, Zeng X (2012) Evaluation of multireanalysis products with in situ observations over the Tibetan Plateau. *J Geophys Res Atmos* (1984–2012) 117(D5):D05102
- Wheatley D, Stensrud D (2010) The impact of assimilating surface pressure observations on severe weather events in a WRF mesoscale ensemble system. *Mon Weather Rev* 138:1673–1694
- Wu TW, Qian ZA (2003) The relation between the Tibetan winter snow and the Asian summer monsoon and rainfall: an observational investigation. *J Clim* 16(12):2038–2051
- Wu GX, Duan AM, Liu YM, Mao J, Ren R, Bao Q, He B, Liu B, Hu W (2015) Tibetan Plateau climate dynamics: recent research progress and outlook. *Natl Sci Rev* 2:100–116
- Xie AH, Allison I, Xiao CD, Wang SM, Ren JW, Qin DH (2014) Assessment of surface pressure between Zhongshan and Dome a in East Antarctica from different meteorological reanalyses. *Arct Antarct Alp Res* 46:669–681
- Yanai MH, Li C (1994) Mechanism of heating and the boundary layer over the Tibetan Plateau. *Mon Weather Rev* 122:305–323
- Yanai MH, Li C, Song Z (1992) Seasonal heating of the Tibetan Plateau and its effects on the evolution of the Asian summer monsoon. *J Meteorol Soc Jpn* 70:319–351
- Yang K, Ye BS, Zhou DG, Wu BY, Foken T, Qin J, Zhou ZY (2011) Response of hydrological cycle to recent climate changes in the Tibetan Plateau. *Clim Change* 109(3–4):517–534. <https://doi.org/10.1007/s10584-011-0099-4>
- Yang K, Wu H, Qin J, Lin C, Tang W, Chen Y (2014) Recent climate changes over the Tibetan Plateau and their impacts on energy and water cycle: a review. *Global Planet Change* 112:79–91
- You QL, Kang SC, Aguilar E, Yan YP (2008a) Changes in daily climate extremes in the eastern and central Tibetan Plateau during 1961–2005. *J Geophys Res Atmos* 113:D07101
- You QL, Kang SC, Pepin N, Yan YP (2008b) Relationship between trends in temperature extremes and elevation in the eastern and central Tibetan Plateau, 1961–2005. *Geophys Res Lett* 35:L04704. <https://doi.org/10.1029/2007gl032669>
- You QL, Fraedrich K, Min J, Kang S, Zhu X, Ren G, Meng X (2013a) Can temperature extremes in China be calculated from reanalysis? *Global Planet Change* 111:268–279
- You QL, Fraedrich K, Ren G, Pepin N, Kang S (2013b) Variability of temperature in the Tibetan Plateau based on homogenized surface stations and reanalysis data. *Int J Climatol* 33(6):1337–1347
- You QL, Sanchez-Lorenzo A, Wild M, Folini D, Fraedrich K, Ren G, Kang S (2013c) Decadal variation of surface solar radiation in the Tibetan Plateau from observations, reanalysis and model simulations. *Clim Dyn* 40(7–8):2073–2086
- You QL, Min J, Zhang W, Pepin N, Kang S (2015a) Comparison of multiple datasets with gridded precipitation observations over the Tibetan Plateau. *Clim Dyn* 45(3):791–806. <https://doi.org/10.1007/s00382-014-2310-6>
- You QL, Min JZ, Lin HB, Kang S, Nick P (2015b) Observed climatology and trend in relative humidity in the eastern and central Tibetan Plateau. *J Geophys Res Atmos* 120:3610–3621
- You QL, Jiang ZH, Moore G, Bao YT, Kong L, Kang SC (2017) Revisiting the relationship between observed warming and surface pressure in the Tibetan Plateau. *J Clim* 30:1721–1737
- Zhao T, Guo W, Fu C (2008) Calibrating and evaluating reanalysis surface temperature error by topographic correction. *J Clim* 21(6):1440–1446. <https://doi.org/10.1175/2007jcli1463.1>
- Zishka KM, Smith PJ (1980) The climatology of cyclones and anticyclones over North America and surrounding ocean environs for January and July, 1950–77. *Mon Weather Rev* 108:387–401

**Publisher's Note** Springer Nature remains neutral with regard to jurisdictional claims in published maps and institutional affiliations.